CLM-P760

CLM-P760

UKAEA

Preprint

# IMPURITY CONTROL AND ITS IMPACT UPON START-UP AND TRANSFORMER RECHARGING IN NET

M. F. A. HARRISON



CULHAM LABORATORY
Abingdon Oxfordshire
1985

CLM-P 760

# IMPURITY CONTROL AND ITS IMPACT UPON START-UP AND TRANSFORMER RECHARGING IN NET

M.F.A. Harrison

Culham Laboratory, Abingdon, Oxon OX14 3DB, U.K.
(Euratom/UKAEA Fusion Association)

ABSTRACT

The present inductive start-up scenarios for NET are, in broad outline, based upon a limiter configuration for the current initiation and ramp-up phases and a divertor configuration for the heating and burn phases. There have been extensive modelling studies of both the boundary plasma conditions and their impact upon impurity control in the burn-phase and these, when coupled to experience in relevant experiments such as JET, facilitate the identification of likely problems during start-up and transformer recharging.

Present knowledge indicates that the inductive start-up scenario appears, with certain caveats, to be compatible with the requirements for impurity control. A particularly significant issue is likely to be the benefit of forming the divertor configuration as soon as possible during start-up. In addition, problems can arise if a limiter plate, constructed from low atomic number material, becomes contaminated with tungsten from the divertor target. In contrast, it seems likely that the transformer recharging scenario could present serious problems.

(Submitted for publication in Proceedings of a Workshop on Tokamak Start-up, Erice, July 1985)

October 1985

## 1. INTRODUCTION

Control of the release of impurities and their subsequent ingress and exhaust from tokamak plasmas has been the subject of intensive studies aimed at both the prediction of reactor burn condition and the interpretation of results from present experiments. In contrast, control concepts which are specific to current-initiation, current ramp-up and RF heating during start-up of a reactor such as NET have to date received but little attention. The requirements for impurity control during the burn phase can be summarised as follows. Firstly, the necessity to dissipate about 80 MW of non-radiated plasma power without incurring either an excessive release of impurities from the plasma collection surfaces or an unacceptable build-up of impurities within the hot reacting core of the D/T plasma. Secondly, the ability to pump neutral helium gas at the rate of about $2 \times 10^{20}$ atoms/s in such a manner that the helium ash concentration within the reacting plasma does not exceed ~ 10%. The level of impurity contamination should neither degrade energy confinement (which implies a maximum concentration of $10^{-3}$ to $10^{-4}$ respectively of medium to high atomic number impurities) nor cause excessve contribution to the plasma $\beta$(which implies a typical concentration of light impurities of $\sim 10^{-2}$). During start-up, the concentration of impurities is not likely to be critical for current-initiation but, especially in the case of high atomic number elements, it becomes significant during the ramp-up and heating phases and it will have a powerful effect upon the ignition margin.

Experience gained from present experiments and from modelling indicates that the predominant sources of impurities arise from plasma-surface interactions and that the properties of the edge plasma and, in particular the scrape-off and divertor plasmas, play significant roles in both impurity release and the subsequent screening of the bulk plasma against the ingress of impurities from boundary surfaces. Conditions in the edge plasma also influence the exhaust of helium ash produced in the burn-phase by D/T fusion reactions.

Sophisticated models of the transport of plasma energy and particles have been developed and linked to models of both plasma-surface interactions and the transport of neutral particles in the edge region. The physics concepts embodied in these models have in large measure been substantiated

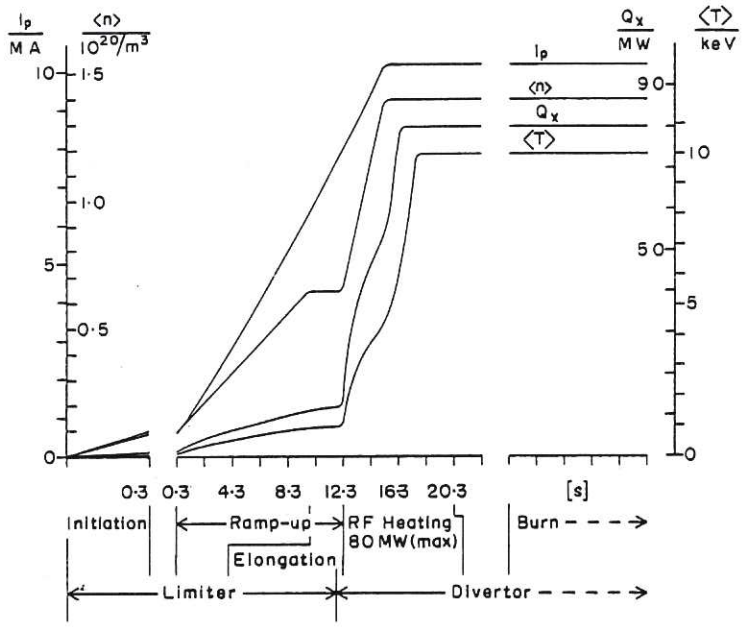


Fig.1 A preliminary concept of the inductive start-up in NET.

The scenario [Cooke[6]] is based on a zero dimensional plasma model. Average density <n> and temperature <T> are derived using prescribed radial profiles and the density limit is taken to be

$$\langle n \rangle_{crit} = (2B_t/Rq_I)10^{20}/m^3.$$

$Q_x$ is the surplus input power, i.e. the amount in excess of inductive losses and the energy dissipated in heating the plasma. Impurity radiation losses are neglected and $Z_{eff}$= 1.5 is assumed.

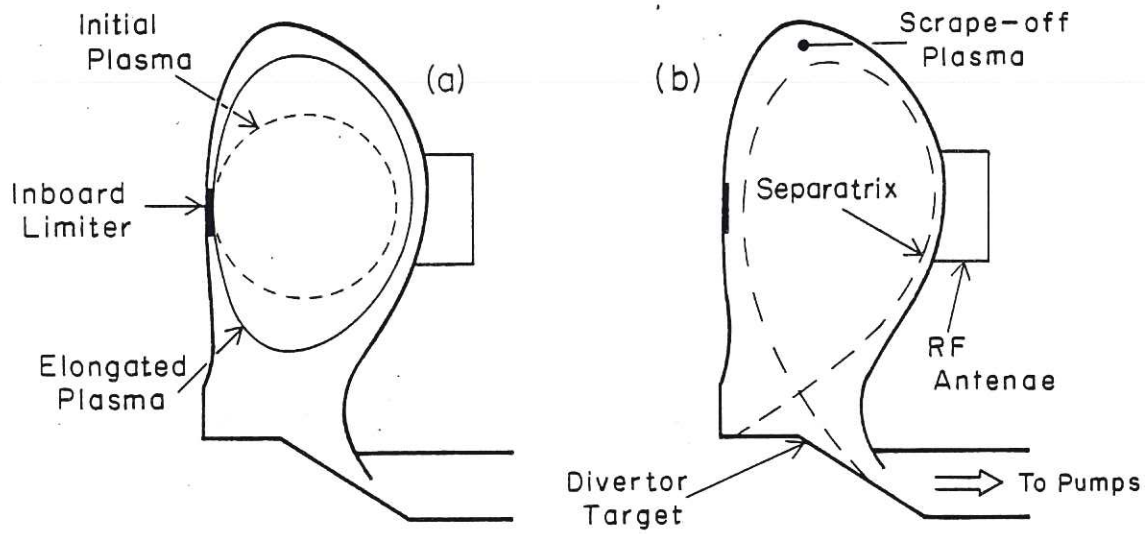


Fig.2 Plasma configurations during start-up

(a) Initially a circular cross section plasma is formed against an inboard limiter; during ramp-up this plasma is elongated.
(b) A single-null divertor configuration is established before RF heating.
A comparable sequence would be adopted in the case of a double-null divertor.

by comparison with experimental results. The present status of model validation is briefly reviewed in Ref. 1 and a comprehensive survey of plasma edge physics, both theoretical and experimental, is available in Ref. 2.

Prediction of plasma edge conditions in the burn-phase (for examples see Refs. 3 to 5) have led to the conclusion that an open throated, poloidal divertor, operated in a regime of powerful but localised recycling of D/T plasma, will provide the most effective means of impurity control and exhaust of helium ash. Furthermore, the use of high atomic number refractory metals (such as tungsten) for the divertor target surface will ensure that the release rate of sputtered impurities will be low and the divertor lifetime commensurately long. Compatibility of this concept with the start-up scenario (and also with the possible application of non-inductive current-drive) has still to be assessed in a quantitative manner. Thus, although the present paper provides an introduction to the relevant background information, its treatment of transient phases is perforce somewhat qualitative. It is expected that the subject will benefit greatly from the existence of closely relevant experiments, particularly JET, TFTR, JT60 and ASDEX-upgrade.

## 2. START-UP AND TRANSFORMER RECHARGING IN NET

The inductive start-up scenario[6] which is illustrated in Fig. 1 is typical of those presently being considered for NET. The phase of ionisation and current-initiation lasts for about 0.3 s during which a circular cross section plasma is formed against a limiter on the inboard side of the first wall. This is indicated in Fig. 2(a). During the ramp-up phase, the plasma current whose initial magnitude is $\sim 0.6$ MA is increased at a rate of 0.6 MA/s in accord with experience gained on JET. Plasma density is also increased from its initial average value of $\langle n \rangle \sim 10^{19}/m^3$ but the rate of rise is so controlled that the density limit is not exceeded. Plasma elongation commences when the safety factor at the edge approaches the value $q_I \approx 2$ which occurs at about 9.8 s. The divertor configuration, shown in Fig. 2(b), is formed at about 12 s when the plasma current has increased to about 70% of its final value of 10 MA. The magnetic separatrix is then moved outward so that it is correctly located with respect to the RF antennae which are mounted on the outboard side of the first wall. Ion cyclotron frequency heating is switched on at about 12.3 s and raised to a maximum power of about 80 MW. This auxiliary heating phase lasts for about 8 s during which ignition is attained. The burn-phase lasts for several hundred seconds during which some variations in plasma conditions due to burn control and fuelling are inevitable. When the burn is terminated both the plasma density and current must be ramped-down prior to the dwell phase between burn cycles.

Uncertainties associated with non-inductive current drive have so far precluded its inclusion in the NET concept but the design will be flexible to the extent that current drive could be incorporated at a later date. The most practicable approach to quasi-steady plasma current is to sustain this current during a transformer recharging phase (of $\sim 100$ s duration) which is interposed between consecutive burn-phases. About 15 MW of lower-hybrid frequency power is required but the plasma density and temperature must be ramped-down to $\langle n \rangle \lesssim 3 \times 10^{18}/m^3$ and $\langle T \rangle \sim 1$ keV in order to attain practicable efficiency.

The start-up scenario involves operation initially with a limiter configuration and finally with a divertor configuration but, even during divertor operation, plasma conditions deviate substantially from those

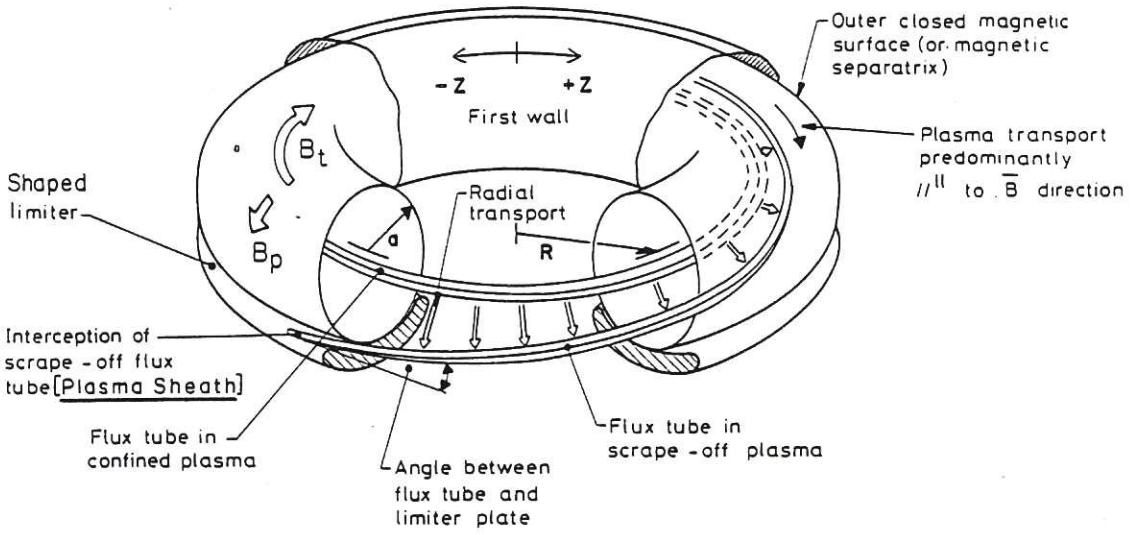


Fig.3 Topography of the scrape-off layer.

The illustration refers to a toroidally symmetric limiter located at the bottom of the torus but the principles are equally applicable to a poloidal divertor.

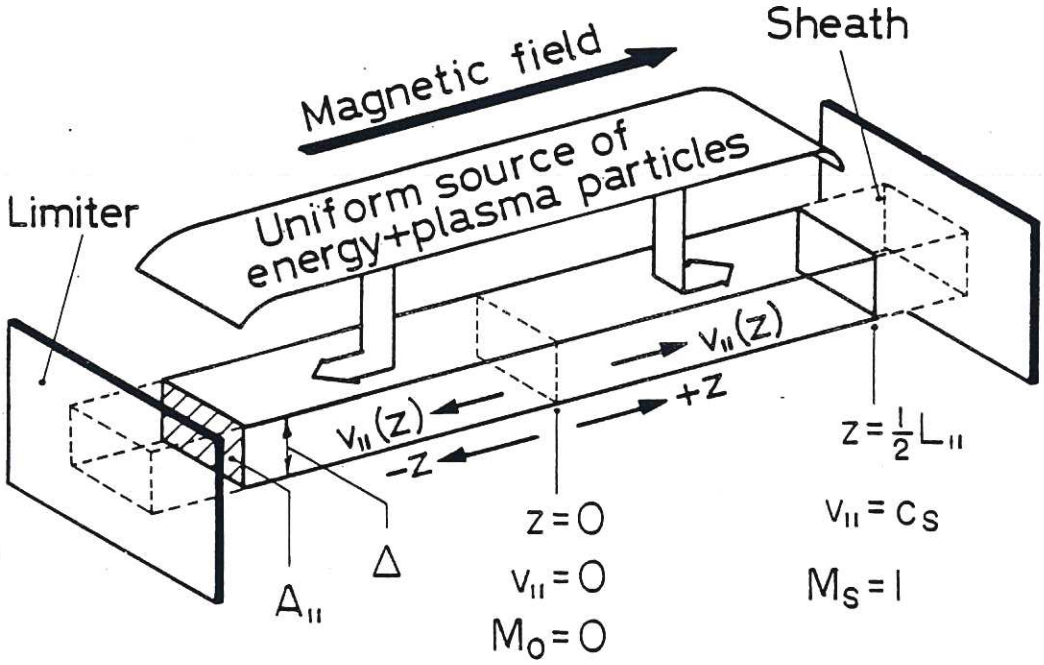


Fig.4 A simplified concept of the scrape-off layer.

The helical flux tube which encompasses the scrape-off region is shown projected along the magnetic field. The inputs of energy and particles from the main plasma are assumed to be uniformly distributed over the face of the flux tube which lies in contact with the main plasma. The parameters are described in the text.

envisaged for the burn-phase. In particular both the average density and the input power are likely to be lower. In order to appreciate the significance of these differences it is first necessary to consider the behaviour of plasma in the edge region and how this influences plasma-surface interactions and thereby impacts upon impurity control.

## 3. PROPERTIES OF THE EDGE PLASMA

### 3.1 Topography

The topography of the edge of a tokamak plasma is illustrated in Fig. 3 which for clarity of presentation shows a toroidally symmetric limiter located at the bottom of the torus. The discussion is, however, general and equally applicable to the poloidal divertor configuration shown in Fig. 2(b). The magnetic surfaces set up by the toroidal ($B_t$) and poloidal ($B_p$) components of the magnetic field are closed inboard of the limiter (or magnetic separatrix in the case of a divertor) but outboard of the limiter or separatrix the surfaces intersect the limiter plate or divertor target. Thermal energy from the main plasma enters this outer ("scrape-off") plasma as a consequence of conduction and convection in the radial direction transverse to the confining magnetic field. The action of the magnetic confinement strongly impedes transport in this direction but it has little influence upon transport of energy by conduction and convection in the direction parallel to the field. Parallel transport within the main plasma does not cause a loss of power or particles because the magnetic surfaces are closed but, in the scrape-off plasma, energy can readily flow along the open magnetic flux tubes to the limiter plate or divertor target.

In the case of a circular cross section plasma of major radius R and a toroidally symmetric limiter (or separatrix) at minor radius a, the length of the open flux tubes which intersect the limiter can be defined as

$$L_{\parallel} = 2\pi R q_a \qquad (1)$$

where $L_{\parallel}$ lies in the direction z parallel to the magnetic field and

$$q_a = \frac{a}{R}\frac{B_t}{B_p} \qquad (2)$$

is this "safety factor" at a.

In a reactor such as NET, the effective mean free paths for collisions between the charged particles within the scrape-off plasma are small relative to the scale of the system (in the z direction) so that collisional conditions prevail and the dominant mechanism for energy transport towards the limiter or divertor is electron thermal conduction parallel to the magnetic field. However this concept of collisional (i.e. fluid) flow cannot pertain at distances comparable to an electron-electron mean free path from the plasma collection surface. Thus, convective transport becomes dominant in the collisionless region of the ion accelerating plasma sheath which forms at this surface.

### 3.2 Plasma Transport

Although detailed analysis of plasma transport requires sophisticated modelling (for example see Ref. 5) an adequate appreciation can be gained from simple concepts. The scrape-off plasma, which is illustrated schematically in Fig. 4, is considered in its projection along the magnetic

field. It is assumed that plasma electrons and ions which diffuse outward from the main plasma and enter the scrape-off layer have equal probability of drifting along the magnetic field in either the positive or negative z directions. The average length of flux tube traversed by the plasma is therefore $\frac{1}{2}L_{\parallel}$.

At a position z, the power $Q_{\parallel,z}$ conducted by electrons along a flux tube of area $A_{\parallel}$ (where $A_{\parallel}$ is the cross section normal to the field) can be expressed as

$$Q_{\parallel,z} = A_{\parallel}\alpha(z)\,\kappa_{\parallel}^{e}\,\frac{dkT_e}{dz}. \qquad (3)$$

Here $kT_e$ is the local electron temperature and $\kappa_{\parallel}^{e}$ is the thermal conductivity, namely

$$\kappa_{\parallel}^{e} = \kappa_o(kT_e)^{5/2} \qquad (4)$$

where $\kappa_o$ [$\approx$ 2000 W $m^{-1}$ ($eV^{-7/2}$) for a clean hydrogen plasma] is the coefficient of Spitzer thermal conductivity parallel to the magnetic field. The function $\alpha(z)$ accounts for the distribution (along the flux tube) of power which enters the scrape-off region from the main plasma. If this power is uniformly distributed in the z direction and $A_{\parallel}$ is constant, then the power, $Q_{\parallel,s}$, conducted to the sheath region at a limiter* can be expressed as

$$Q_{\parallel,s} = \frac{4}{7}A_{\parallel}\kappa_o\left[(kT_o)^{7/2} - (kT_s)^{7/2}\right]/\tfrac{1}{2}L_{\parallel}. \qquad (5)$$

The plasma temperature at the upstream location where the flow is stagnant (at z = 0) is $kT_o$ and that at the sheath boundary (at $x = \pm \frac{1}{2}L_{\parallel}$) is $kT_s$. Even a modest temperature gradient renders $kT_o^{7/2} > kT_s^{7/2}$ and so, to a reasonable degree of approximation,

$$kT_o \approx \left[\frac{7\,Q_{\parallel,s}\,L_{\parallel}}{8\,A_{\parallel}\,\kappa_o}\right]^{2/7}. \qquad (6)$$

The upstream temperature $kT_o$ is therefore only weakly dependent upon plasma parameters and indeed $kT_s$ = 100 to 200 eV embraces both present day experiments and NET.

The downstream boundary temperature $kT_s$ is determined by the ability of the sheath to convect to the limiter (or to the divertor target) that amount of energy which flows into the sheath by conduction along the scrape-off layer. This self consistent sheath condition can be expressed as

$$Q_{\parallel,s} = \Gamma_{\parallel,s}A_{\parallel}\gamma_s kT_s = n_s v_{\parallel,s}A_{\parallel}\gamma_s kT_s \qquad (7)$$

where $\Gamma_{\parallel,s}$ is the flux of ion-electron pairs which enter the sheath and $\Gamma_{\parallel,s} = (n_s\, v_{\parallel,s})$ where $v_{\parallel,s}$ is the plasma drift velocity and $n_s$ the plasma density at the sheath boundary. The coefficient $\gamma_s$ describes the amount of

---

* Equation (5) is slightly modified in the case of a poloidal divertor to allow for the additional length of the flux tube which lies within the divertor and which receives no radial input of power from the main plasma. This distinction is neglected in the present simple discussion.

energy deposited upon the surface by each ion-electron pair which traverses the ion accelerating sheath. The magnitude of this coefficient ($\gamma_s$= 5 to 7) is discussed in Section 4.1. It is reasonable to assume that $v_{\parallel,s}$ is equal to the ion sound speed, $c_s$, at the sheath boundary and so for ions of charge state Z and mass $m_i$,

$$v_{\parallel,s} = c_s = \left(\frac{ZkT_i + kT_e}{m_i}\right)^{\frac{1}{2}} \qquad (8)$$

thus, when Z = 1 and ($kT_i = kT_e = kT$),

$$Q_{\parallel,s} = n_s A_\parallel \gamma_s kT_s \left(\frac{2kT_s}{m_i}\right)^{\frac{1}{2}}. \qquad (9)$$

The crucial role played by the plasma sheath potential $U_s \approx (3\ kT_s/e)$ in controlling impurities released due to sputtering of the plasma collection surface by plasma ions is discussed in Section 4.2. Suffice to state here that it is advantageous for the temperature $kT_s$ not to exceed about 40 eV and it is envisaged that, during heating and burn, this relatively low value will be attained due to localised enhancement of the ion flux [$\Gamma_{\parallel,s}$ in Eq. (7)] which arises as a consequence of powerful recycling of neutral D/T close to the divertor target. The maximum degree of recycling is however restricted because an upper limit is imposed upon the local plasma density ($n_s$) due to the properties of fluid plasma flow along the scrape-off layer. Conditions of fluid flow require that the pressure $n_s kT_s$ at the sheath boundary be linked to its upstream value $n_o kT_o$ at the point of flow stagnation (i.e. at x = 0) by the relationship

$$\frac{n_o}{n_s} = \frac{(1 + M_s)^2\ T_s}{(1 + M_o)^2\ T_o} = \frac{2T_s}{T_o} \qquad (10)$$

where the Mach number ($v_\parallel/c_s$) is $M_s \approx 1$ at the sheath and $M_o = 0$ at the stagnation point. It is thus possible to rearrange Eq. (9) in the form

$$kT_s = \left(\frac{m_i}{2}\right)\left[\frac{Q_{\parallel,s}}{kT_o}\,\frac{q_a}{\gamma_s}\,\frac{1}{2\pi a \Delta n_o}\right]^2 \qquad (11)$$

where cross sectional area $A_\parallel$ has been replaced by the geometrically equivalent thickness, $\Delta$, of the flux tube which encompasses the energy scrape-off layer (i.e. $2\pi RqA_\parallel = 4\pi^2 Ra\Delta$).

The thickness of the scrape-off layer is small (~ few x $10^{-2}$ m in NET) because electrons transport heat much more readily along the magnetic field than across it. Following the approach in Ref. 7, the characteristic radial decay length of power flow can be written as

$$\Delta = \left[\chi_\perp\ \tau_\parallel/3\right]^{\frac{1}{2}} \qquad (12)$$

where the containment time $\tau_\parallel$ refers to energy losses along the field and can be determined from

$$\tau_\parallel = \frac{3\ n_s\ kT_s\ (4\pi^2 Ra\Delta)}{Q_{\parallel,s}}\ . \qquad (13)$$

Here the numerator is the energy stored in the scrape-off length $\frac{1}{2}L_{\parallel}$ and the denominator is the power flow lost to the limiter or divertor target. Manipulation yields

$$\Delta = \left(\frac{2\pi R q_a \chi_{\perp}}{\gamma_s}\right)^{1/2} / \left(\frac{2kT_s}{m_i}\right)^{1/4} \qquad (14)$$

which shows that $\Delta$ is rather insensitive to plasma parameters and that the values found in present experiments such as ASDEX, PDX and Doublet III are not expected to differ substantially from those in NET.

It is convenient to summarise this analysis by noting that both the upstream temperature $kT_o$ and the scrape-off thickness $\Delta$ are rather insensitive to plasma parameters. A useful guide to the properties of the scrape-off plasma is thus given by

$$kT_s \propto \left[\frac{Q_{\parallel,s}}{n_o}\frac{q_a}{\gamma_s}\right]^2. \qquad (15)$$

For a particular surface material $\gamma_s$ tends to be only weakly dependent upon $kT_s$ over the temperature range of interest. In contrast, considerable variation in the ratio $(Q_{\parallel,s}/n_o)$ is envisaged for the various transient phases of NET operation and the commensurate variation of $kT_s$ can (as discussed in Section 4.2) have a powerful effect upon the sputtering of the limiter or the divertor target. Indeed the impurity control concept for the heating and burn phases is strongly dependent on attaining values of $n_o$ that are not substantially less than $5 \times 10^{19}/m^3$.

### 3.3 Boundary Plasma Conditions during the Burn and Heating Phases

In order to predict plasma-boundary behaviour to the precision needed for design specifications it is necessary to undertake a much more comprehensive analysis. Transport of plasma energy and particles must be considered in directions both along and across the magnetic field and contributions to transport from convection, friction and the presence of electric fields within the drifting plasma must be accounted for. The influence of power losses due to atomic radiation must be assessed and the influence of magnetic topography and the effects of the geometry of the first wall, divertor chamber and pumping ducts taken into account.

A typical set of predictions[5] for the burn-phase of a reactor such as NET is illustrated in Fig. 5. An ab initio assumption is that about 30% of the $\alpha$-particle heating power is lost from the main plasma by radiation but the remaining power, about 80 MW, must be transported to a single-null poloidal divertor. The analysis is therefore also indicative of the plasma condition likely during the heating phase. Radial transport coefficients are assumed to be anomalous and based upon present experimental data (namely, thermal diffusivity $\chi_{\perp} = 2\ m^2/s$ and diffusion $D_{\perp} \approx 0.5\ \chi_{\perp}$). A critical input parameter is plasma density at the separatrix which is here assumed to be about 0.3 $\langle n \rangle$, namely $5 \times 10^{19}/m^3$. This particular calculation is based on a rather high value of plasma $\beta$ ($\approx 4.6\%$) and, as a consequence, there is compression of the scrape-off layer at the outer equatorial plane. This can be seen in Fig. 5(a). This compression in conjunction with other poloidal asymmetries which arise from the D-shape of the plasma causes a lack of symmetry in the scrape-off plasma which links the inner and outer divertor targets and this in turn causes the power flow to the outer divertor to be about 1.7 times greater than that to the inner. Localised recycling of D/T within the divertor (which is discussed in detail

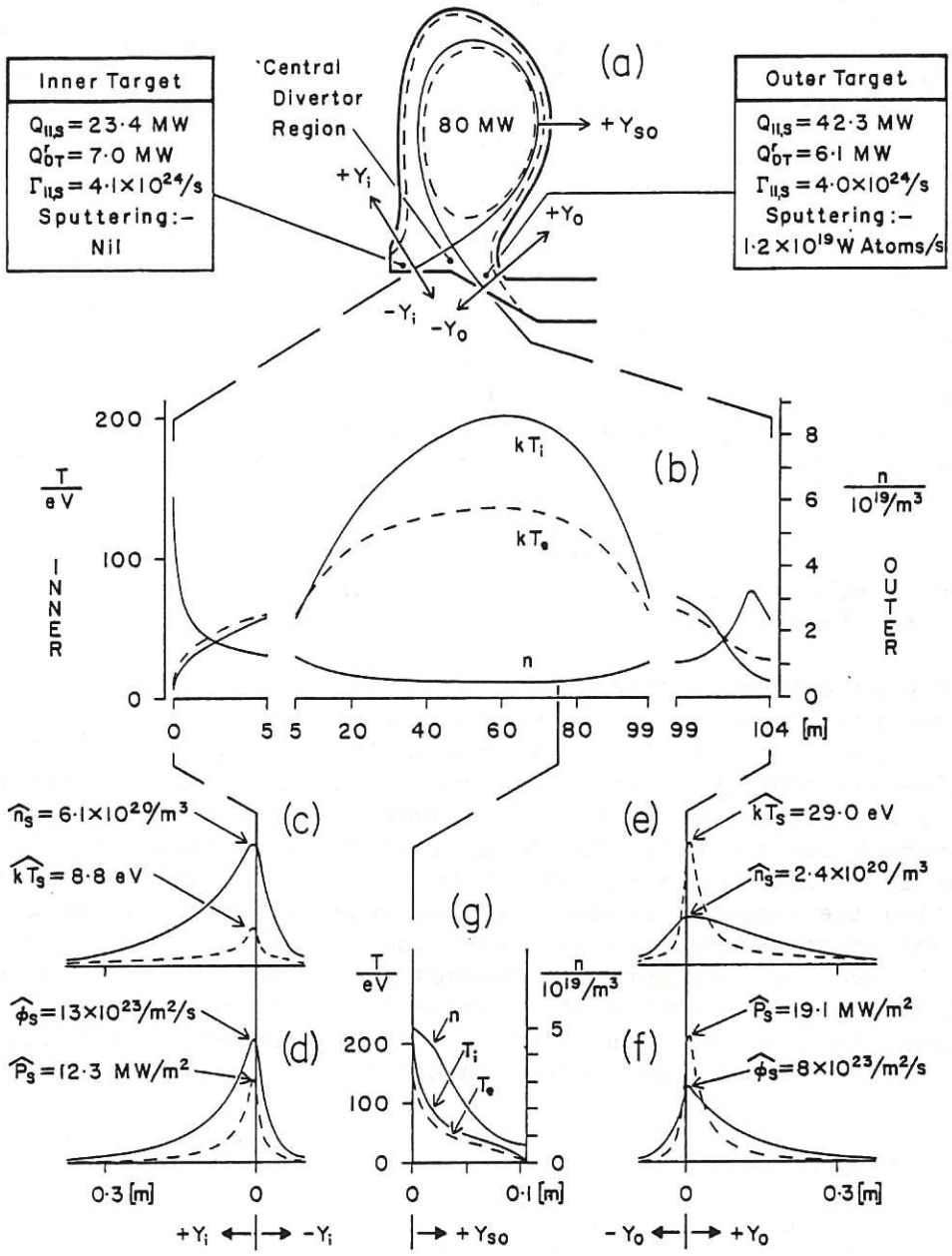


Fig.5 Predicted behaviour of the scrape-off and divertor plasma in a NET like device[5]

(a) shows the non-circular main plasma and single-null divertor. Modelling is based upon a 2-dimensional, fluid description of plasma transport and this is coupled to a model of neutral particle transport within the divertor.
(b) Shows variation of $kT_e$, $kT_i$ and n with distance along the magnetic field at the separatrix.
(c) and (e) show the radial profiles of $n_s$ and $kT_s$ (in the direction perpendicular to the magnetic surfaces) at the inner and outer targets respectively.
(d) and (f) show the corresponding radial profiles of plasma flux density and target power loading.
(g) shows the radial profiles of $kT_i$, $kT_e$ and n at the mid equatorial plane. Here the scrape-off layer is compressed due to the rather high value of plasma $\beta(\sim 4.6\%)$.

in Section 4.3) dissipates about 13 MW by atomic radiation but the remaining plasma power is deposited upon the divertor targets. The magnetic surfaces in the scrape-off region are expanded within the divertor chamber and this helps to reduce the peak power load at the divertor target. The peak power load is also significantly reduced by diffusion of plasma energy into the central region of the divertor but, even so, the outer divertor target must be inclined at about 10° to 15° to the magnetic surfaces in order to reduce the peak load to an acceptable level of about 5 $MW/m^2$.

Figure 5(b) shows the variation of n and kT along the separatrix and it is evident that the simple concepts discussed in Section 3.2 are upheld. The radial profiles of $kT_s$ and $n_s$ at the inner divertor target are shown in Fig. 5(c) and the associated radial profiles of the plasma particle flux density and power density in Fig. 5(d). The corresponding conditions at the outer target are shown in Figs. 5(e) and 5(f) where it is evident that the maximum value of $kT_s$ ($\approx$ 30 eV) occurs at the outer target. The benefit of this low temperature in controlling of impurity sputtering is discussed in Section 4.2. Radial profiles of $kT_o$ and $n_o$ in the scrape-off region at the outer equatorial plane are presented in Fig. 5(g) and their significance upon impurity release due to the impact of charge exchange atoms upon the first wall is discussed in Section 4.6.

The choice between a single-null or double-null poloidal divertor for the NET conceptual design has not yet been made. Modelling of the plasma edge for various configurations has however identified a number of trends. In a single-null configuration, the asymmetry of power flow caused by poloidal asymmetries enhances the peak power loading at the outer target. A useful approach for reducing this power load is to increase the plasma triangularity by moving the null-point to a smaller major radius. In such a configuration the magnetic surfaces in the outer divertor are more strongly expanded and there is commensurate reduction in peak power loading. A double-null divertor configuration removes the asymmetry in the scrape-off layer and so power is shared equally between the upper and lower divertors. Nevertheless, the reduction in scrape-off length causes a significant increase in the plasma temperature adjacent to the divertor targets.

## 4. IMPURITY CONTROL

### 4.1 The Incident Energy of Plasma Ions

The plasma sheath sets up an ion accelerating potential difference between the surface and the plasma in order to maintain ambipolar conditions at the downstream boundary of the scrape-off plasma. This potential, whose magnitude in the case of cold, singly charged ions, can be expressed as

$$U_s \approx \frac{kT_e}{2e} \ln \left(\frac{m_i}{2\pi m_e}\right) \qquad (16)$$

is only slightly dependent upon the fact that the toroidally symmetric surface of the limiter or divertor lies at grazing incidence to the direction of the magnetic field[8]. It can however be influenced by the emission of secondary electrons from the surface but these electrons are effectively suppressed by the grazing magnetic field and, for D/T ions, $U_s \approx (3kT_e/e)$ can be taken as a reasonable value. Ions of charge state Z which enter the ion accelerating sheath with a Maxwellian distribution of velocities corresponding to $kT_i$ impact upon the surface with a kinetic energy

$$E_i \approx 2kT_i + ZeU_s \qquad (17)$$

whereas electrons impact with kinetic energy

$$E_e \approx 2kT_e. \qquad (18)$$

However, not all of this energy is deposited upon the surface. The boundary material quickly becomes saturated with D/T atoms (i.e. after a fluence of $\sim 10^{22}$ ions/m$^2$) and in this conditions there is negligible absorption of incident ions. The arrival of each ion is therefore accompanied by the release of a particle and most of these are neutral. Depending on the particular combination of surface material, ion species and incident energy, a significant fraction, $R_N(E_i)$, of the incident ions are on average backscattered in the form of energetic neutral atoms. On average, these carry away from the surface a fraction $R_E(E_i)$ of the incident particle energy so that the average energy of the backscattered atoms is $R_E/R_N$. The remaining fraction of neutral particles $(1 - R_N)$ tend to be molecules whose kinetic energy probably corresponds to the temperature of the surface. The coefficients $R_N$ and $R_E$ for carbon and tungsten are shown in Fig. 6.

The energy deposited upon the surface by each D/T ion-electron pair is thus

$$E_{ie} = (1 - R_E)E_i + E_e + \chi_i \qquad (19)$$

where $\chi_i$ (= 13.6 eV) is the stored potential energy of $D^+$ and $T^+$ which is released when the ions recombine at the surface. The transport coefficient $\gamma_s$ introduced in Eq.(7) can thus be defined as

$$\gamma_s = E_{ie}/kT \qquad (20)$$

and, for values of $R_E$ and $kT_s$ envisaged for NET, the magnitude of $\gamma_s$ lies in the range 5 to 7.

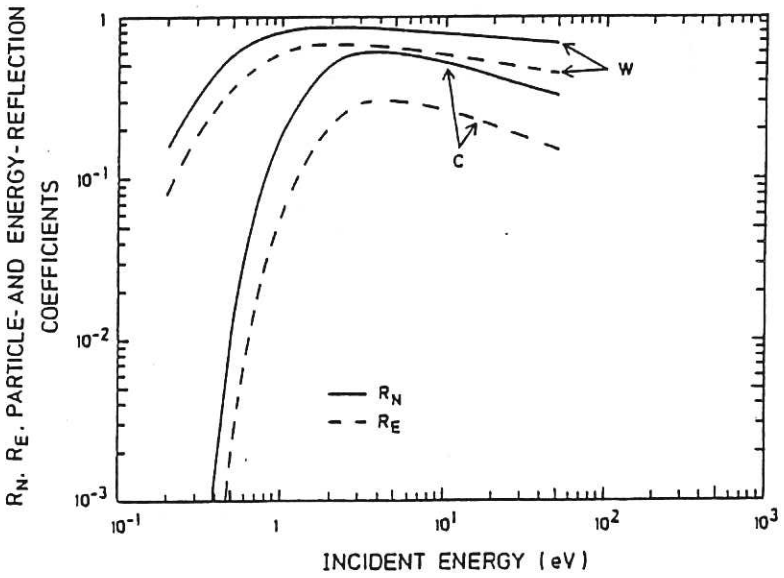


Fig.6 Particle ($R_N$) and Energy ($R_E$) reflection coefficients for carbon and tungsten surfaces.

Data are for normal incidence and are taken from Ref.9.

## 4.2 Sputtering by Plasma Ions

The flux of plasma ions to either the limiter or divertor target greatly exceeds the flux to other regions of the boundary and so sputtering of these surfaces is expected to be the most likely source of impurities. The physical sputtering yields* for carbon, stainless steel and tungsten are presented in Fig. 7. The marked differences in the sputtering threshold energies are apparent, i.e. (13 eV for T→C), (37 eV for T→SS) and (140 eV for T→W). The sputtering threshold for tungsten is so high that, if the plasma temperature at the sheath edge can be maintained in the range $kT_s$ = 20 to 40 eV, the rate of sputtering is very small. This fact implies that tungsten (or a comparable refractory metal) is a good choice for the divertor target of NET even though the powerful atomic radiating properties of tungsten ions imposes a limit of about $10^{-4}$ upon their concentration within the plasma core. A further consequence of this powerful temperature dependence is that the radial profile of tungsten sputtering is much more narrow than the profiles of either $kT_s$ and or $n_s$ [whose typical forms can be seen in Figs. 5(e) and 5(f)]. The width of the sputtering profile during burn is expected to be only 2 to 3 x $10^{-2}$ m. In the case of a divertor, frequent excursions of the divertor plasma channel caused by uncertainties in position control are likely to smear out the erosion profile and thereby reduce the erosion peak[5]. It should however be noted that this beneficial action does not occur at a limiter.

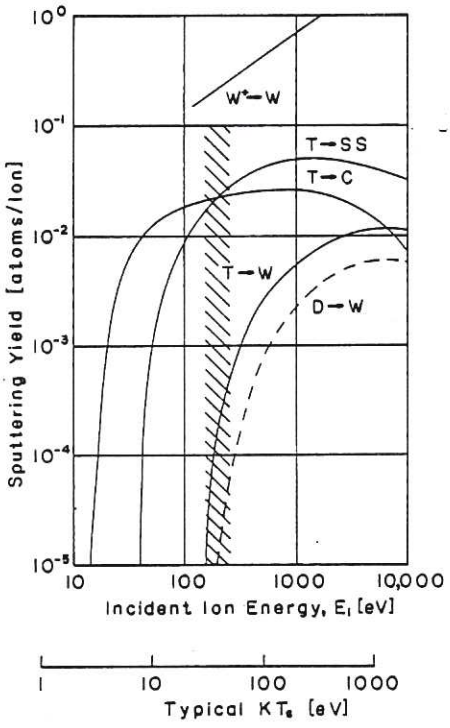


Fig.7 Yields for physical sputtering of carbon, stainless steel and tungsten by tritons and deuterons incident normally on the surface[10].

Also shown is the self sputtering yield for tungsten on tungsten. The shaded region indicates the regime of plasma temperature which is compatible with a tungsten target.

---

* The term "physical sputtering" refers to interactions involving momentum exchange between the incident ion and the lattice atoms. Contributions from additional processes such as the formation of methane on carbon surfaces are not illustrated.

In addition to D/T ion sputtering, it is necessary in the case of heavy metals to consider the consequences of self-sputtering and so the yield for $W^+$ ions on tungsten is shown in Fig. 7. Sputtered tungsten atoms enter the plasma and, as will be described in Section 4.4, recycle to the sheath with charge states greater than unity. Accepting that the average charge state is $\langle Z \rangle \approx 4$ implies, from Eq.(17), that the self-sputtering yield approaches a cascading threshold (i.e. where the yield is unity) when $kT_s \rightarrow 60$ eV. Thus there is a relatively small window in $kT_s$ in which operation with a tungsten divertor target is acceptable.

The adaption of medium atomic number targets such as stainless steel appears to be impracticable because both the D/T sputtering threshold and the self-sputtering threshold are low. Alternatives to tungsten are the low atomic number elements such as carbon or beryllium and possibly such materials as SiC and TiC. Although self-sputtering of these materials is much reduced, it is unlikely that the sheath temperature in NET can be reduced below the $D^+/T^+$sputtering threshold. The physical sputtering rates are thus expected to be at least $\sim 10^2$ times that of tungsten. Most of the sputtered atoms return to the target but there must be some spatial re-distribution of the return flux so that the surface profile of the target (and hence its local power loading) are changed. There is concern that the operational lifetime of such targets may be too short for practicable application in NET. In the case of carbon, whose surface will be very hot, additional processes such as chemical sputtering and ion induced evaporation will exacerbate the problem[11].

The presence of even small concentrations of light impurity ions in the edge plasma can significantly enhance the sputtering rate because, (a) these ions are more massive than D/T and have an intrinsically higher sputtering yield, (b) they become multiply-charged and are thus more strongly accelerated by the sheath and (c) frictional forces exerted by the drifting D/T plasma tend to increase the energy of these ions prior to their entry into the sheath (see Section 4.4). In the burn-phase it is impossible to eliminate helium but its contribution to sputtering appears to be acceptable[5] and moreover it is not present in significant quantities during start-up. It is however highly desirable to eliminate oxygen ions because of the powerful chemical sputtering that they introduce. Small concentrations ($\sim 1\%$) of carbon can probably be tolerated.

## 4.3 Localised Recycling

During burn in a clean plasma, the power transported from each end of the scrape-off layer to the plasma collection surface in NET is about 40 MW and a somewhat reduced power flow is envisaged during the heating phase. In order to maintain $kT_s \lesssim 30$ eV, a flux of plasma particles to the surface, $\Gamma_{\parallel s} \gtrsim 5\times10^{24}$ ions/s, is required. This flux cannot be sustained by the radial flow, $\Gamma_\perp$, of particles which diffuse from the main plasma into the scrape-off plasma. This radial flow can be expressed as

$$\Gamma_\perp \sim D_\perp \frac{dn_o}{dr} A_p \qquad (21)$$

where $D_\perp$ ($\sim 1$ m$^2$/s) is the anomalous radial diffusion coefficient and $A_p$ is the surface area of the main plasma. For likely values of the radial density gradient ($dn_o/dr$), the outward radial flux in NET does not exceed $\sim 10^{23}$ ions/s. Fortunately, the ion flow parallel to the magnetic field is enhanced by natural processes once the plasma collector has become saturated with D/T. Neutral D/T particles, which are then backscattered or detrapped from the material, are re-ionised quite close to the surface when the local

values of $n_s$ and $kT_s$ lie in the regime envisaged for NET. The range of D/T atoms, $\lambda^o$, is of the form[12],

$$\lambda^o \sim \left[\frac{S_{cx}(kT_i)}{3S_i(kT_e)}\right]^{\frac{1}{2}} \lambda_{cx}(kT_i) \qquad (22)$$

where $\lambda_{cx}(kT_i)$ is the mean free path for charge exchange. $S_{cx}(kT_i)$ and $S_i(kT_e)$ are respectively the rate coefficients for charge exchange with plasma D/T ions and for ionisation by plasma electrons and these are shown in Fig. 8. The magnitude of $\lambda^o$ in NET is typically less than $10^{-2}$ m. This range is greater than the thickness of the sheath so that re-ionisation occurs in the adjacent plasma. The re-ionised particles tend to share their momentum and energy with the plasma which is already flowing to the surface. They thereby become entrained in the plasma flow and so return, via the ion accelerating sheath, to the surface. The cycle is repeated until such time as the neutral particle escapes by being pumped from the system. The localised recycling sequence in a divertor is illustrated, in a highly schematic fashion, in Fig. 9.

It is convenient to characterise localised recycling by a coefficient

$$R_s \approx (\Gamma_{\parallel,s} - \Gamma_\perp)/\Gamma_{\parallel,s} \qquad (23)$$

and it is useful to note, that for steady state conditions, a neutral particle flux (equal in magnitude to $\Gamma_\perp$) must be pumped from the system. In the case of the open throated, single-null divertor envisaged for the burn and heating phases of NET, most of the neutral particles (whose flux $\Gamma^o \approx \Gamma_{\parallel,s}$) are re-ionised directly whilst they are traversing the divertor plasma channel. A relatively small fraction are re-ionised indirectly after rebounding from the chamber wall back into the plasma. A recycling coefficient, $R_s > 0.99$ is expected[5]. The small flow of pumped neutrals (equivalent to a few x $10^{-3}$ $\Gamma_{\parallel,s}$) is adequate to exhaust the helium ash produced during burn.

Localised recycling at a limiter is inherently less substantial due to the unavoidable escape of neutrals into the closed field region which lies in contact with the limiter surface[13,14] The recycling coefficient at a limiter during the burn-phase of NET is unlikely to exceed $R_c \sim 0.8$ and, unless atomic radiation losses from the main plasma are large (~ 70%), the peak plasma temperature at the sheath will be in the region of 100 eV.

The presence of large quantities of recycling neutral D/T helps to dissipate some of the incident plasma power in the form of atomic radiation. When the target material is saturated with gas (i.e. when $\Gamma^o \approx \Gamma_{\parallel,s}$), the power radiated by D/T can be expressed as

$$Q^r_{DT} \approx R_s \Gamma_{\parallel,s} E^r_{DT}(n_e, kT_e). \qquad (24)$$

Here $E^r_{DT}(n_e,kT_e)$ is the average amount of radiated energy associated with the life history of each recycling D/T atom and the dependence of $E^r_{DT}$ upon plasma electron density and temperature can be seen in Fig. 10. The power dissipated in the divertor due to D/T neutrals in the burn-phase of NET is relatively small; the modelling reported in Fig. 5 predicts $Q^r_{DT} \approx 13$ MW out of a total input of about 80 MW to the divertor. The fraction of energy dissipated by radiation tends to increase when the power flowing along the scrape-off plasma is decreased because $E^r_{DT}$ increases with decreasing $kT_s$.

When the thickness ($\sim \Delta$) of the divertor plasma is larger than the atomic range $\lambda^o$, most recycling occurs due to direct ionisation and little

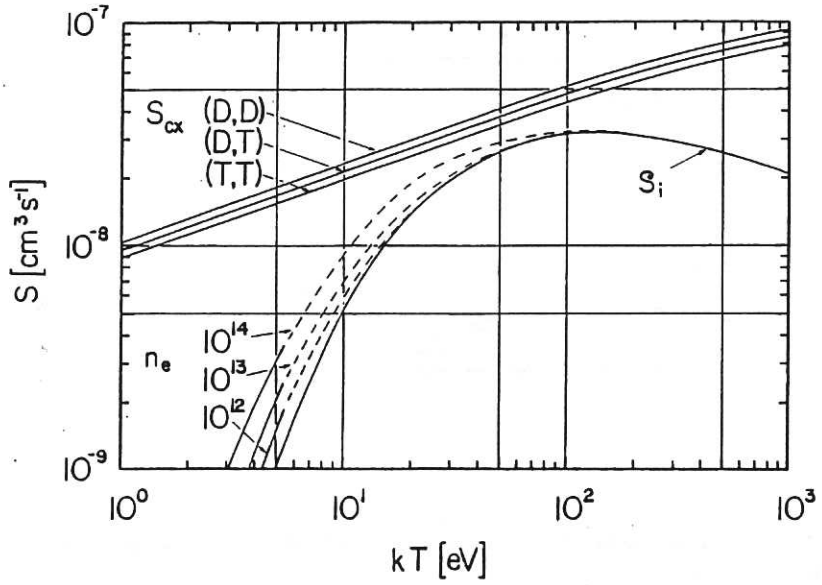


Fig.8 Rate coefficients for charge exchange and electron ionisation of D/T atoms.

The ionisation rate coefficient $S_i(kT_e)$ is enhanced at higher electron densities[12] and data for $n_e = 10^{12}$, $10^{13}$ and $10^{14}/cm^3$ are plotted.

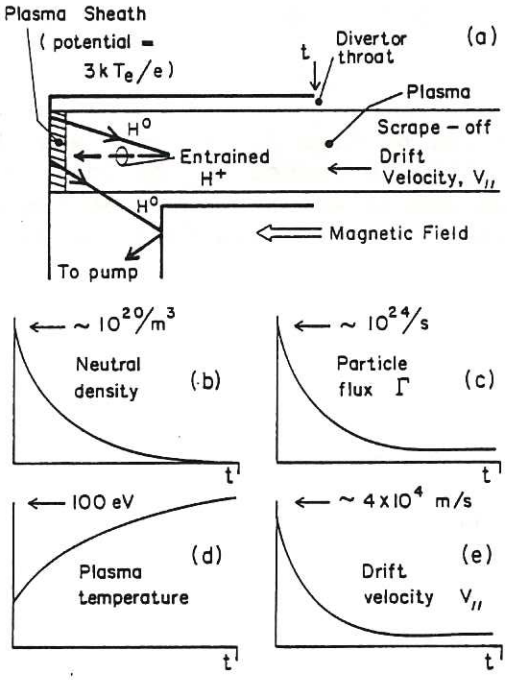


Fig.9 Highly schematic representation of localised recycling within a divertor chamber.

(a) Plasma environment projected in the direction of the magnetic field (note that the inclination of the target is not shown); (b) Density of neutral D/T; (c) Flux of plasma ions; (d) Plasma temperature and (e) Plasma drift velocity.

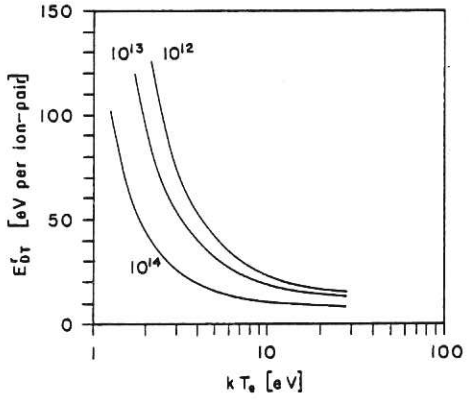


Fig.10 The average radiation energy $E_{DT}^r$ dissipated during the life of a recycling D/T atom.

Data from Harrison[12] are plotted for plasma densities $n_e = 10^{12}$, $10^{13}$ and $10^{13}/cm^3$.

energy is dissipated by atoms which reach the chamber wall. An approximate equality in power lost to the target and power lost by atomic processes then occurs when the plasma power flowing to the target is just adequate to sustain a sheath temperature of about 10 eV because at this temperature the equality

$$\gamma_s kT_s \approx (\chi_i + E_{DT}^r) \qquad (25)$$

is satisfied. In conditions of high power flow, when $kT_s > [(\chi_i + E_{DT}^r)/\gamma_s]$, it is, in principle, possible to reduce $kT_s$ by introducing an additional flow ($\Gamma_g^o$) of D/T gas into the divertor and thereby enhancing the ion flux to the target. Manipulation of Eqs. (9) and (10), assuming that $kT_o \sim$ (constant), yields

$$n_o \propto (\Gamma_\perp + \Gamma_g^o)^{\frac{1}{2}} \qquad (26)$$

for conditions when the plasma power flow into the divertor is constant and the gas flow is introduced in such a manner that its recycling coefficient similar in magnitude to $R_s$. The additional gas flow must not be so large that the enhanced $n_o$ exceeds the density limit and also that the vacuum pump can be capable of handling the additional gas load. At lower power flows ($\sim$ 10 MW) it may be possible to reduce $kT_s$ to $\sim$ 5 eV but, in this regime, there is a tendency for the temperature to become clamped because the strongly non-linear behaviour of $\lambda^o(kT_e)$ causes the recycling gas to be ionised in the neighbourhood of the 5 eV isotherm. Only tentative assessments of additional gas feed during the burn of NET have been made and the results indicate that a rather modest reduction in $kT_s$ may be practicable. Even so, the reduction in sputtering of a tungsten divertor target could be substantial.

Power losses by atomic processes tend to predominate in present high recycling divertor experiments and this can be explained by the relatively low levels of input power and of divertor plasma density. There are several significant consequences of these conditions. Firstly, the divertor plasma temperature tends to be clamped in the 5 eV regime. Secondly, because $\lambda^o > \Delta$, the energetic neutrals which are backscattered from the target

deposit their energy on the chamber wall rather than returning it to the plasma. Thirdly, the plasma is but marginally collisional and the effective parallel thermal conductivity may be significantly less than the Spitzer value.

An important feature of localised recycling is its influence upon the plasma drift velocity $v_{\parallel}(z)$. The one-dimensional fluid equation for continuity is

$$\frac{d}{dz}(nv_{\parallel}A_{\parallel}) = SA_{\parallel} \qquad (27)$$

where S is the volume source term (particles/$m^3$/s). The volume source in the scrape-off plasma is dependent upon $\Gamma_{\perp}$ but in the region of localised recycling S depends upon $\Gamma^{o}$ and it is thereby increased by a large factor ($> 10^2$ in NET). It is evident from fluid flow analyses (for example Ref.15) that the velocity gradient ($dv_{\parallel}/dz$) is dependent upon (S/n) so that the gradient is small within the scrape-off and very large within the recycling region. The boundary conditions for $v_{\parallel}$ are that the Mach number of the plasma flow is $M_o = 0$ at the upstream stagnation region and $M_s = 1$ at the sheath edge. In the conditions envisaged for the NET divertor the Mach number of the plasma flow will not exceed $M \sim 10^{-2}$ except in the extreme downstream region where localised recycling occurs and where it will increase rapidly to its boundary value of $M_s = 1$. This very marked variation in M(z), is illustrated schematically in Fig. 9(e). It is expected to impact strongly upon the impurity retention and impurity exhaust capabilities of the divertor.

## 4.4 Retention and Exhaust of Impurities by a Divertor

It is envisaged that the divertor target in NET will be separated by about 0.5 m from the main plasma so that any neutral impurity released from the target will be ionised within the divertor. However, in order that these ions be retained, it is necessary for them to be entrained in the drifting D/T plasma and returned to the target. A comparable argument applies to the exhaust of impurities released from the first wall into the scrape-off plasma. Entrainment of an impurity ion (with charge state Z) depends upon a balance of forces[15,16], the most significant are:

(i) Friction forces which act towards the target; these are proportional to $Z^2$ and to the difference between the impurity ion velocity and the D/T plasma drift velocity, i.e. $v_{\parallel}(z)$.

(ii) Thermal diffusion which is proportional to $Z^2$ and to the ion temperature gradient ($dT_i/dz$). The force, as can be infered from Fig.5(b), is directed away from the target and towards the stagnation region of D/T plasma flow.

(iii) Electric field forces which are proportional to Z and to the plasma pressure gradient (dP/dz), in general the electric field accelerates ions towards the target but there can be regions of local field reversal.

A convenient criterion[16] which identifies the dominance of friction (and hence of entrainment) for ions of moderately high Z is,

$$M > \lambda_{ii}/\lambda_T \qquad (28)$$

where $\lambda_{ii}$ is the mean free path for Coulomb collision between impurity ions and D/T plasma ions and $\lambda_T$ is the scale length of the ion temperature

gradient. This criterion can be applied to the one-dimensional concept (evolved in Section 4.3) for the variation of the Mach number with distance along the magnetic field and the following behaviour can be identified[16]. Those impurities which are ionised close to the target in the region of powerful D/T recycling where M is large, for example sputtered target atoms, will be returned to the target. Their residence time within the plasma is short and so their average charge state when re-entering the sheath is quite low, $\langle Z \rangle \sim 4$. If impurities enter the divertor plasma upstream of the D/T recycling region where M is small, then the forces tend to be balanced and impurity ion flow tends to stagnate. There is a local accumulation of impurities and diffusion from this local peak in concentration re-distributes the ions both towards the target and towards the scrape-off plasma. The retention within the divertor is thus degraded. The ion residence time is relatively long so that ions arrive at the sheath edge in relatively high charge states and with velocities that approach the $D^+/T^+$ ion sound speed. When the impurity ions are massive, this entrainment implies that the ions are subjected to very considerable acceleration prior to their final acceleration in the plasma sheath. This mode of transport is particularly relevant to gaseous impurities which may rebound from the divertor chamber wall and then become ionised in the plasma close to the divertor throat. It may explain the rather poor retention efficiency for non-condensible gases (i.e. oxygen, neon, etc.) observed in experiments. The residence time of impurities released into the scrape-off plasma distant from the divertor will be even longer and whether they are exhausted into the divertor or are returned to the first wall by radial diffusion depends strongly on the radial properties of the scrape-off plasma.

An appreciation of particle transport both along and across the open regions of magnetic field is provided by two-dimensional modelling such as that described in Ref. 5. On the one hand, this model demonstrates that the simple picture so far evolved here for $v_{\parallel}(z)$ is valid in the recycling region close to the target and also in the outermost scrape-off layer (close to the first wall). On the other hand, it indicates that particle flow near

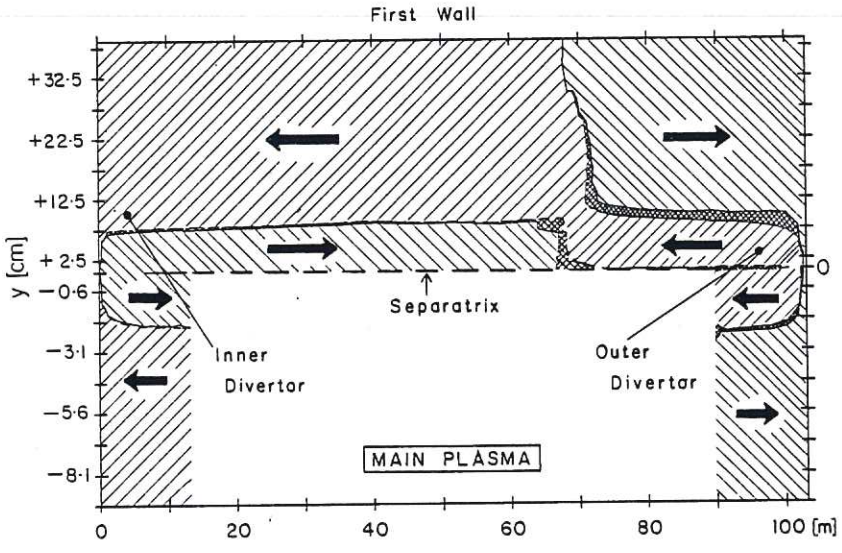


Fig.11 A two-dimensional plot of the impurity entrainment criterion.

The criterion[16] is applied to data from Ref. 5. For clarity of presentation, variation in scrape-off thickness is not shown. Arrows show the direction of the D/T plasma flow and hence the direction of entrainment. Cross hatching shows regions where the impurity flow will tend to stagnate.

to the separatrix is much more complex because circulating flow regions are formed upstream of the recycling region. At the divertor throat, the flow of D/T plasma close to the separatrix is directed outward into the scrape-off region but, within the scrape-off region, circulation forces the flow to stagnate and then be directed radially outward so that it returns to the divertor along the outermost region of the scrape-off plasma. Application of the entrainment criterion given by Eq. (28) to the flow pattern predicted by a two-dimensional transport model[5] yields the results shown in Fig. 11. The following trends can be identified:

(i) Atoms released from the divertor target will be well retained within the divertor.

(ii) Helium ions entering the scrape-off region from the main plasma may be impeded in their transport towards the divertor until circulation has re-directed them to the outermost region of the scrape-off plasma.

(iii) Impurities released from the first wall will in general be directed towards the divertor because the ionisation mean free path ($\approx 5 \times 10^{-2}$ m) lies within the outermost scrape-off region where flow is directed towards the divertor. The ion transit time to the divertor is $\sim 10^{-2}$ s and, because the radial scale-length for outward diffusion ($\approx 0.1$ m) is comparable to the ionisation mean free path, most of these impurities will return to the first wall rather than be exhaused into the divertor.

## 4.5 Impurity Retention by a Limiter

The principles of impurity retention discussed in the context of a divertor are also applicable to a limiter but the overall retention of impurities is dominated by the different magnetic configuration. The closed magnetic surfaces lie in contact with the limiter and a significant fraction of the neutral particles released at the limiter surface, either as a result of recycling or of sputtering, must enter the main plasma. Localised recycling is therefore inherently less effective in reducing sputtering and sputtering per se is inherently more liable to cause atomic radiation losses together with wasteful enhancement of the plasma $\beta$ and increased plasma $Z_{eff}$. In the case of a divertor, the main plasma is likely to be relatively clean so that radiation losses are expected to be modest (about 30%) and plasma edge conditions are thus largely governed by parallel transport within the scrape-off and divertor plasma. Reasonable confidence can therefore be placed in predictive modelling. However, in the case of a limiter, the penetration of strongly radiating impurities into the main plasma will significantly reduce the plasma power transported along the scrape-off plasma to the limiter. There is, in principle, a self-regulating cycle. An increase in the release of impurities causes an increase in radiation which in turn reduces the plasma power in the scrape-off region and hence the sheath temperature and thereby the rate of impurity release. Indeed, this concept of a cool radiating mantle[17] has been invoked as a possible scenario for limiter operation. Results from one such analysis[18] for carbon, iron and tungsten limiters in JET with 28 MW of RF (or $\alpha$-particle) heating are shown in Fig. 12. In the case of tungsten, about 50% of the input power is radiated and a significant fraction of this emanates from the hot plasma core. With an iron limiter, about 75% of the input power is radiated but a much smaller fraction emanates from the hot plasma core. For carbon, only 25% of the input power is radiated and the loss from the plasma core hardly exceeds that of bremsstrahlung radiation from the pure D/T plasma.

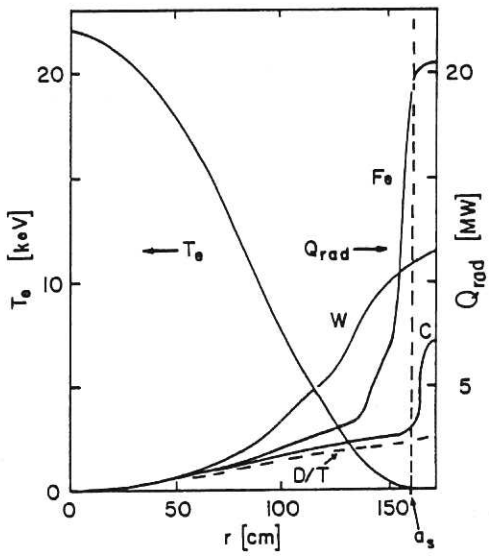


Fig.12 Radial characteristics of radiated power losses caused by carbon, iron and tungsten limiters.

Data are taken from[18] and refer to JET with 28 MW of RF (or α-particle) heating.

Despite these apparently encouraging results, it must be stressed that the detailed behaviour is extremely sensitive to the radial transport properties assumed for both impurities and D/T plasma. There is concern that either radiation losses from the hot fusion region will be unacceptably high during the ignition and burn-phases or else the cool edge region will penetrate into the plasma to such an extent that the volume available for fusion reactions will become unacceptably small. The present view is that the risk of degraded plasma performance is unacceptable unless the limiter surface consists of a weakly radiating material such as beryllium or carbon and, even then, the increase in plasma β is questionable. Moreover, the sputtering rates of low atomic number materials during the burn-phase are high and the ability to retain the profiled shape of the limiter surface (which is essential to ensure acceptable peak power loading) is very strongly sensitive to any displacement in the redeposition pattern of the sputtered limiter material. Thus, although a low atomic number limiter material may be acceptable (and probably unavoidable) during the current-initiation and the current ramp-up phases, it is unlikely that the limiter can be retained during the RF heating and burn phases. The high probability of cross contamination between the material of the limiter surface and any different material exposed to the plasma has been demonstrated in many experiments and the question of materials compatibility between a limiter used during current-rise and a divertor used during the auxiliary heating and burn-phases has yet to be ascertained.

### 4.6 Impurities from the First Wall

The scrape-off plasma is likely to be quite cold in the vicinity of the first wall (typically a few eV) so that sputtering due to ion impact is not expected to be significant. Possible exceptions arise from the relatively small number of energetic ions produced in the edge during auxiliary heating and also from those superthermal ions (and particularly α-particles) which escape from the main plasma. When the wall has become saturated with gas, the incident D/T ions return to the plasma as cold neutral particles.

Additional cold neutrals are introduced into the plasma edge during fuelling. Motion of neutrals is unimpeded by the magnetic field and so they penetrate radially into the edge plasma until such time as they are ionised or else undergo charge exchange with $D^+$ and $T^+$ ions. The charge exchange reaction for an H atom[‡] with a plasma proton ($H_p^+$) is of the form

$$H + H_p^+ \rightarrow H^+ + H_p^*$$

where $H_p^*$ denotes the daughter atom whose energy is that of the plasma proton but whose velocity tends to be randomly oriented. It is evident from Fig. 8 that the rate coefficient for charge exchange is larger than that for ionisation and, because the daughter atoms move in random directions, a significant fraction (20 to 30%) of the ingoing atom flux returns to the first wall in the form of quite energetic atoms. The rebounding neutrals re-enter the edge plasma and the cycle continues until the atoms are ionised. The distribution of energy amongst the daughter atoms depends upon the radial profile of plasma ion temperature in the region traversed by the atoms. The penetration range, which is of the form shown in Eq. (22), is about 0.1 m for the edge density envisaged for the heating and burn-phases of NET. The velocity distribution shown in Fig. 13 has been predicted[19] using radial profiles of edge plasma density and temperature which are rather similar to those predicted for the burn-phase and shown for the mid equatorial plane in Fig. 5(c). About 15% of the incident atoms are predicted to have energies in excess of 40 eV and 5% have energies greater than 100 eV. The rate of wall sputtering is quite low, about $5 \times 10^{17}$ atoms/m$^2$/s in the case of stainless steel so that the rate of wall erosion (even when redeposition is neglected) is only ~ 0.1 mm/y at 100% availability. Moreover this estimate probably represents a peak rate of sputtering because

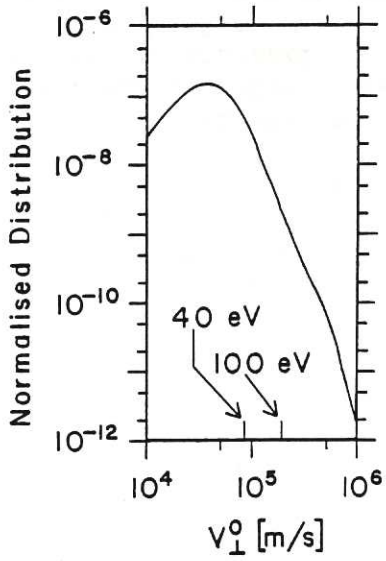


Fig.13 The normalised distribution of the perpendicular velocity ($v_\perp^0$/total incident atom flux) of charge exchange atoms at the first-wall.

Data which are taken from Goedheer[19] refer to a NET-like plasma edge during the burn-phase.

‡ The argument is equally valid for the isotopes D and T.

the scrape-off layer is thinnest at the mid equatorial plane so that the gradient ($dT_i/dr$) is at its maximum. The design requirements of the plasma facing surface of the first wall of NET are therefore likely to be dominated by the consequences of damage due to plasma disruptions rather than by erosion due to charge exchange atoms. Even so, the release rate at a stainless steel wall is so large that a retention efficiency of about 90% is required in the plasma edge region.

## 5. IMPURITY CONTROL DURING AN INDUCTIVE START-UP SCENARIO

Issues related to start-up can be divided into two separate categories, namely operation with a limiter during both current-initation and ramp-up and operation with a divertor during RF heating, ignition and burn. The difference between the magnetic configurations is obvious but the distinction is much more widely routed. During limiter operation, a relatively small amount of plasma power flows along the scrape-off layer and, at least in the early stages, plasma density is relatively low. Moreover, there is now a growing base of closely relevant data on plasma-limiter performance from experiments such as JET. In contrast, prediction of conditions during divertor operation entails a rather large extrapolation from existing experimental results although it can be argued that plasma behaviour is likely to be less sensitive to uncertainties in modelling and that the models per se are likely to be more precise.

### 5.1 Operation with a Limiter

The properties of electric field breakdown of neutral D/T gas dictate conditions during the initial ionisation phase. Losses of free electrons due to formation of negatively charged impurity ions can influence the breakdown characteristics and some likely impurity atoms have quite strong electron affinities e.g. $C^-$, $O^-$, $Cl^-$, etc. However, their impurity concentration in the filling gas is likely to be low and the consequences of electron loss are not expected to be significant. During current initiation, radiation losses due to the presence of impurities will increase the transient demand for transformer energy but the overall degradation of performance is not expected to be important.

During ramp-up of plasma current and density the fraction of input energy dissipated by impurity radiation is likely to be large (in excess of 50%). Experience in relevant devices (e.g. JET and TFTR) indicates that heavy impurity ions cannot be tolerated, at least in the early stages of ramp-up. The reason is not clearly understood but it is possible that the ohmic power is not adequate to sustain the power losses due to impurity radiation at the plasma edge and that this causes the plasma either to collapse or to disrupt. It would thus appear that a low atomic number limiter material is required at this stage, for example, carbon in JET and TFTR and possibly beryllium in NET. The surface of the first-wall should ideally consist of the same material and, furthermore, the potential release of impurities due to sputtering by oxygen should be minimised by removing oxygen from the device. The approach adopted by JET (and TEXTOR) is to coat both the limiter and first-wall with carbon by means of a carbonisation technique which buries heavy impurities and also seals off oxygen. After such treatment and with an ohmic power of about 3 MW, the discharges in JET contain 1 to 2% of carbon and about one tenth of this amount of oxygen; the $Z_{eff}$ is about 2 and about 50 to 70% of the input power is radiated from the plasma edge (see Ref.20).

Whether these constraints and conditions extend throughout the ramp-up scenario is not yet clear. The inductive start-up conditions which have

been tentatively proposed by Cooke[6], and which are shown in Fig. 1, can be taken as an indication of the time dependence of average plasma density $\langle n \rangle$ and of surplus input power $Q_x$. (This surplus power is the amount by which the input power exceeds both the inductive losses and the energy dissipated by heating the plasma). In this particular scenario the ratio $(Q_x/\langle n \rangle)$ increases to a peak value at about 10 s when its magnitude is about twice that at the start of the ramp-up phase. Equation (15) indicates the sheath temperature will increase as the ratio $(Q_x/\langle n \rangle)$ increases. A crude assessment of plasma conditions at the start of ramp-up (based on the assumption that localised recycling to the limiter is minimal at this time) indicates that the sheath temperature is about 40 eV. It is evident from Fig. 7 that the sputtering yield of carbon (and the behaviour of beryllium is comparable) does not increase substantially as the sheath temperature increases over the range of present interest. Although the analysis is crude, it nevertheless predicts a carbon concentration of about 1% which is in accord with JET results. It is expected that this concentration will not be substantially enhanced during the ramp-up phase despite the fact that ion flow to the limiter increases during ramp-up. The reason is twofold, firstly, the efficiency of impurity retention within the scrape-off plasma increases as edge density increases (due to decreasing ionisation mean free path) and, secondly, the cooling effect arising from localised recycling at the limiter also increases with plasma density.

The performance of a limiter constructed of medium or heavy materials is more obscure. There is a very strong increase in sputtering yield as the sheath temperature increases but this is in some measure compensated by an increase in radiative power losses from the plasma edge. The situation is further complicated by the increase in ohmic power with increasing $Z_{eff}$. In view of the present lack of understanding it seems advisable to minimise risks by ensuring that medium or high atomic number materials are not exposed to direct contact with the plasma during limiter operation.

## 5.2 Operation with a Divertor

The divertor configuration is formed before the termination of the ramp-up phase. Depending upon the amount of radiation, the power flow to the divertor will be in the range 5 to 12 MW and no difficulty is foreseen in establishing high recycling conditions when the plasma density at the separatrix in the scrape-off is about $1 \times 10^{19}/m^3$. It is envisaged that the divertor target surface will be tungsten (or a comparable refractory metal) in order that it be compatible with burn conditions but, at this stage, it is expected that the sheath temperature will be well below the sputtering threshold. The divertor action is likely to reduce considerably the level of impurities which will have built-up in the plasma during the earlier ramp-up period. Experimental evidence indicates that the reduction is likely to be greatest for "condensible" impurities (e.g. metals and possibly carbon). Present divertor experiments are less effective in reducing non-condensible gases, oxygen, neon, etc. but this situation is likely to be improved in NET because the divertor will be actively pumped.

The RF heating requirements of NET lie in the range 50 to 80 MW and are typically about half of the $\alpha$-particle heating power envisaged during burn. Modelling predicts that, at full RF power, it will be essential to ensure that the plasma edge density approaches the magnitude expected during burn conditions (i.e. $n \gtrsim 5 \times 10^{19}/m^3$ at the separatrix) in order to sustain an adequate level of recycling within the divertor. To explore this condition modelling has been undertaken[21] for conditions of low separatrix density (6 to $12 \times 10^{18}/m^3$) and rather low plasma power flowing into the divertor, i.e. 20 MW. The results are illustrated here in Fig. 14 by the dependence of the tungsten target sputtering rate upon separatrix density. At higher density

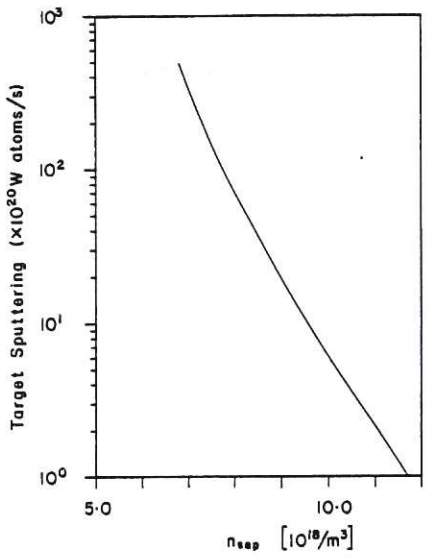


Fig.14 Dependance of the sputtering rate of a tungsten divertor target with density at the separatrix. Data taken from Ref.21 refer to a power flow of 20 MW into the divertor.

the sputtering rate is comparable to that during the burn-phase but, when the density is halved, this rate increases by a factor of about 700. Clearly it is important to tailor the RF power to the plasma density in order to control the release of impurities.

During the burn-phase it is expected that about 80 MW of plasma power will flow along the scrape-off layer into the divertor and that the plasma density at the separatrix is expected to be about $5 \times 10^{19}/m^3$. Accurate prediction of the sputtering rate of the divertor target is not practicable because of the high sensitivity of the yield upon plasma temperature in the regime close to the sputtering threshold, nevertheless, the range 1 to $5 \times 10^{19}$ atoms/s appears to be realistic for a tungsten target. The retention efficiency for impurities within the divertor should thus be at least 95% in order to ensure that the concentration of tungsten in the hot core of the main plasma does not exceed $\sim 10^{-4}$. The ionisation mean free path for tungsten atoms in the divertor is typically less than $10^{-3}$ m whilst for the D/T is typically about $2.5 \times 10^{-2}$ m. Thus tungsten will be ionised well within the region of powerful, localised recycling and, as discussed in Section 4.4, high retention efficiency can be expected.

## 6. TRANSFORMER RECHARGING

It is envisaged that transformer recharging in NET could take place whilst the plasma current is maintained at close to its burn-value by means of about 15 MW of lower-hybrid RF current-drive. The divertor would remain operative but the plasma density would be ramped-down to $\langle n \rangle \sim 3 \times 10^{18}/m^3$ (which implies $n \sim 10^{18}/m3$ at the separatrix) and the plasma temperature to $\langle T \rangle \sim 1$ keV. The evidence presented in Fig. 14 indicates that these conditions will cause a very substantial increase in the sputtering rate of a tungsten divertor target. An efficient transformer recharging cycle requires that plasma resistivity during the drive period be greater than that at the end of the burn. Thus in this respect, the enhancement of $Z_{eff}$ due to an increased impurity concentration during the drive-phase is beneficial. However, whether the level of impurity release from the

divertor could be compatible has yet to be ascertained but it appears to be too great. The recharging phase is expected to last for ~ 100 s so that the divertor target would be subjected to very substantially enhanced sputtering for a considerable fraction of its operational life. The sacrificial thickness of the tungsten surface must thus be commensurately increased and there is a strong possibility that the target lifetime, which for the burn-phase is governed by cyclic thermal stress and hence upon target thickness, will become unacceptably short. It would appear that transformer recharging poses very serious problems in the field of impurity control.

## 7. CONCLUSIONS

Assessment of both the physics and engineering issues related to impurity control during the transient phases of tokamak reactor operation is still in an embryonic stage. There are, however, extensive studies which relate specifically to the steady state burn-phase so that likely problems in the transient phases can be identified even though quantitative analyses are not yet available. On the basis of present knowledge, the envisaged inductive start-up scenario appears, with certain caveats, to be compatible with the requirements of impurity control. Particularly significant issues are the advantages of forming the divertor configuration at the earliest practicable stage and the problems expected due to contamination of the limiter with divertor material. In contrast, it seems likely that the transformer recharging scenario could present serious problems.

## REFERENCES


1. "International Tokamak Reactor Phase Two (part 2)", IAEA Vienna, Ch.III, to be published.
2. "Physics of Plasma-Wall Interactions in Controlled Fusion", eds. R. Behrisch and D. E. Post, NATO ASI, Val-Morin, Canada (1984), to be published by Plenum Press.
3. M. F. A. Harrison, P. J. Harbour and E. S. Hotston, Nucl. Technology/ Fusion, 3: 432 (1983).
4. M. F. A. Harrison and E. S. Hotston, "Predicted Behaviour of the Single-null Divertor in INTOR", Report CLM-R226, Culham Laboratory (1982).
5. M. F. A. Harrison, E. S. Hotston and A. De Matteis, "Plasma Edge Physics for NET/INTOR", to be published as a NET Report (1985).
6. P. I. H. Cooke, private communication (1985).
7. P. J Harbour, Nucl. Fusion, 24: 1211 (1984).
8. R. Chodura "Plasma Flow in the Sheath and the Presheath of a Scrape-off Plasma", in Ref.2.
9. R. Behrisch and W. Eckstein, "Ion Backscattering from Solid Surfaces", in Ref.2.
10. J. Bohdansky (1982) in "European Contribution to the INTOR-Phase IIA Workshop", Euratom, EUR FU BRU/XII-132/82/ EDV30, Brussels (1982), Vol.2, p.VI-319.
11. J. Roth, J. Bohdansky and K. L. Wilson, J. Nucl. Mater., 111/112: 775 (1982).
12. M. F. A Harrison, "Atomic and Molecular Collisions in the Boundary Plasma", in Ref.2.
13. M. F. A Harrison and E S Hotston, "Predicted Behaviour of the Pumped Limiter of INTOR, Report CLM-R232, Culham Laboratory (1982).
14. M. Petravic, D. Heifetz and D. Post., Plasma Phys, Controlled Nucl. Fusion Res., Proc. Int. Conf., 10th, London, UK, 1984.
15. P. J. Harbour and J. G. Morgan, 11th European Conf. on Controlled Fusion and Plasma Physics, Aachen, 1983; EPS 7D Part II (1983) 427.

16. J. Neuhauser, W. Schneider, R. Wunderlich and K. Lackner, J. Nucl. Mater., 121: 194 (1984).
17. A. Gibson, J. Nucl Mater., 76/77: 92 (1978).
18. J. Neuhauser, K. Lackner and R. Wunderlich, "1-D Tokamak Simulation with Self-Consistent Description of Hydrogen Recycling and Impurity Balance" in "European Contributions to the INTOR Phase IIA Workshop", Euratom, EUR FU BRU/XII - 132/82/EDV30, Brussels (1982), Vol.2, p.VI-47.
19. W. J. Goedheer, in "European Contributions to INTOR Phase IIA (Part 2) Workshop", Vol.2, p.III-107, to be published by Euratom.
20. A. Gibson, in "Conf. Rep. on 3rd European Tokamak Fusion Workshop", Athens, Dec. 1984, to be published in Plasma Physics and Controlled Fusion.
21. M. F. A Harrison and E. S. Hotston, in "European Contributions to INTOR Phase IIA (Part 2) Workshop", Vol.2, p.III-117, to be published by Euratom.